Journal of Sound and Vibration
Volume 290, Issues 1-2, 21 February 2006, Pages 34-47

Noise-induced synchronization of uncoupled nonlinear systems

Katsutoshi Yoshida *, Keijin Sato , Atsushi Sugamata

Department of Mechanical Systems Engineering, Utsunomiya University
7-1-2 Yoto, Utsunomiya-shi, Tochigi 321-8585, Japan
TEL: +81-286-89-6005 ext.6071 / FAX: +81-286-89-6009
E-Mail: yoshidak@cc.utsunomiya-u.ac.jp (Katsutoshi Yoshida)

Abstract

We derive a recursion formulae of transition probability of the noise-induced synchronization arising in a pair of identical uncoupled logistic maps linked by common noisy excitation only. The formulae has a delta-type stationary solution which represents the perfect synchronization with probability 1. The stationary solution maintains under chaotic bifurcation while the escape times to reach the perfect synchronization increase in the chaotic region. The escape times analysis implies existence of lower dimensional dynamics around the perfect synchronization. We also provide a physical implementation of the synchronization.

1 Introduction

One of the most surprising results of the last few decades in the field of the nonlinear dynamics is that a dynamical system and its copies can be synchronized with each other when they are linked by the common excitation only. For instance, the main idea of the chaotic synchronization resides in sending the output of a driving system to response systems of the same structure whose conditional Liapunov exponents are all negative[1,2]. Recently, stochastic counter parts of the chaotic synchronization have also been developed, showing that common excitations as elements of the original system are not necessary to produce the synchronization and can be replaced by external noisy signals. This kind of noise-induced synchronization of the dynamical system with its copies can easily be found in nonlinear systems, such as the discrete maps[3,4], the Lorenz system[3], the Duffing oscillator[5], the single mode CO_2 laser[6], and the uncoupled neurons[7]. One of the

* Corresponding author.

most important results in these studies is that the perfect synchronization may arise under some suitable conditions[3,5,6]. Moreover, it also must be noted that the perfect synchronization exhibits significant degree of robustness against mismatches in the copies such as the parameters mismatch[5] and the independent random fluctuation of the copies[3,8].

Stability of the synchronization has been explored in terms of the error dynamics[9,10]. Fujisaka[9] proposed the general stability theory to characterize relationship between the coupling strength and non-synchronized motion. Kim[10] estimated the critical parameter value for the onset of on-off intermittency. These studies mainly focus on the coupled synchronization or the master-slave interaction of coupled systems. In contrast to these studies, the stability for uncoupled case has also been investigated by Pikovsky[11]. He investigated uncoupled one-dimensional noisy maps and derive the scaling law of statistics of trajectory separation. In addition, as another approach from random dynamical systems point of view[12], we have already reported that the noise-induced perfect synchronization of the van der Pol systems, the Duffing systems, and the nonlinear retarded systems can be characterized by point attractors of random invariant measures[8,13], showing that if the system and its copy are subjected to a common sample path of the noisy excitation, their orbits belonging to the different coexisting fixed points (or attractors), which are produced by the Hopf bifurcation[8,13], the saddle-node bifurcation, and pitchfork bifurcation[8], lose their sensitivity of initial conditions, and consequently becomes perfectly synchronized.

In these studies, however, the main interest involves long time behaviour of target systems to characterize dynamical aspects of the synchronization, so that it seems that only a few sample paths of the excitation are of interest in their investigations. This means that little attention has been given to the question as to whether the synchronization occurs over all the sample paths of the excitation. To solve this problem, Maritan and Banavar[14] employed the Fokker-Plank equation of a pair of randomly forced continuous-time nonlinear systems to provide rough estimation of existance of stationary joint probability distribution of the form $\delta(x-y)\exp(-\beta V(x))$, which confirms the perfect synchronization of the pair of continuous-time systems.

In contrast to the continuous-time case above[14], we focus on a pair of uncoupled discrete-time systems and propose a recursive description of the perfect synchronization arising in the pair. Our description will provide a discrete-time counterpart of the Fokker-Plank description given by Maritan and Banavar[14]. From an engineering point of view, we mainly focus on periodic response of the pair. That is, the perfect synchronization of the periodic pair implies that one can synchronize coexisting engineering oscillators of the same specification by adding a common noisy input only, instead of performing accurate setup of initial conditions of the oscillators. In this paper, we first investigate stochastic properties of the noise-induced synchronization arising in a pair of identical uncoupled logistic maps linked by common noisy excitation only. Although the same system has al-

ready been studied by Maritan and Banavar[14] and Rim et al[15], it seems that their stochastic results on the logistic maps, obtaining the mean square distance or probability densities of error dynamics, are computed from Monte-Calro simulations. In contrast, we regard the response of the discrete maps as a Markov process and derive the joint probability density of it in a recursive form. We then analytically show that the Markov process has an absorbing barrier which corresponds to the perfect synchronization. The analytical result is in good agreement with that of Monte Carlo simulations. We also provide numerical estimations of mean escape times and show that extent of attraction of the absorbing barrier are changed under chaotic bifurcations. Furthermore, presence of lower dimensional dynamics around the perfect synchronization is shown numerically and analytically. Finally, we propose a physical implementation of the noise-induced synchronization and demonstrate the nearly perfect synchronization arising in a pair of multivibrators linked by a common noisy input only.

2 Noise-induced synchronization

2.1 Synchronization of the logistic maps

We consider a synchronization system composed by a pair of identical uncoupled logistic maps linked by common noisy excitation of the following form:

$$\begin{aligned} x_{n+1} &= A_n x_n(1 - x_n), \\ y_{n+1} &= A_n y_n(1 - y_n) \end{aligned} \tag{1}$$

where A_n is the noisy term which is uniformly distributed in the interval $[A_c - \sigma, A_c + \sigma]$. If $\sigma = 0$, then the system (1) coincides the deterministic logistic map with the constant parameter $A_n = A_c$ $(\forall n)$. In order to determine the range of σ to be considered, the bifurcation diagram of the one-dimensional logistic map:

$$x_{n+1} = Ax_n(1 - x_n) \tag{2}$$

is shown in Figure 1. From the diagram, we choose the centre value $A_c = 10/3$ and strict the value of σ in the range $0 \leq \sigma \leq 0.2$ to avoid the one-periodic domain, $A < A_0 \approx 3$, in which the trivial synchronization of the system (1) occurs.

Figure 2 shows a sample process of the synchronization system (1) whose noise intensity σ is changed from 0 to 0.2 at $n = 30$. In the deterministic case for $n < 30$, the two-periodic responses x_n, y_n of different initial values oscillate with the phase difference of period one. As σ is changed to 0.2 at $n = 30$, the responses x_n, y_n become synchronized with each other.

For further investigation, we introduce the transformation:

$$\begin{bmatrix} r_n \\ s_n \end{bmatrix} = \begin{bmatrix} 1 & -1 \\ 1 & 1 \end{bmatrix} \begin{bmatrix} x_n \\ y_n \end{bmatrix}.$$

Then, the original equation (1) is rewritten as

$$\begin{aligned} r_{n+1} &= A_n r_n (1 - s_n), \\ s_{n+1} &= A_n \Big(s_n - \frac{r_n^2 + s_n^2}{2} \Big) \end{aligned} \tag{3}$$

where $r_n = x_n - y_n$ represents error of the synchronization. In what follows, we refer to the new equation (3) as an error system of the synchronization system (1).

2.2 Stability of the error system

We first examine the case for the fixed $A_n = A_c$ $(\forall n)$. Based on the linearized form of the error system (3) given by

$$\begin{bmatrix} \delta r_{n+1} \\ \delta s_{n+1} \end{bmatrix} = \begin{bmatrix} A_c(1 - s_n) & -A_c r_n \\ -A_c r_n & A_c(1 - s_n) \end{bmatrix} \begin{bmatrix} \delta r_n \\ \delta s_n \end{bmatrix},$$

the stability of the period two points of (3) is obtained. All the stable period two points for $A_c = 10/3$ are listed below.

Index	Period two point	Eigenvalue
FP1	$(0, (13 \pm \sqrt{13})/10)$	$-4/9$
FP2	$(\pm \sqrt{13}/10, 13/10)$	$-4/9$

The trivial (FP1) and the nontrivial (FP2) solutions correspond to the synchronized and the unsynchronized responses of the error system (3) respectively. It is clearly shown that both the synchronized and the unsynchronized solutions have the same eigenvalue $-4/9$ which is a stable eigenvalue of discrete maps. Therefore, in the deterministic case, there is no difference in stabilities between the synchronized and the unsynchronized solutions.

By contrast to the deterministic case, the nontrivial solution (FP2) loses its stability in the stochastic case where A_n is random. Figure 3 shows a sample process of the error system (3) starting from the nontrivial solution (FP2). The noise intensity σ is changed from 0 to 0.2 at $n = 30$. In the deterministic case for $n < 30$, the nontrivial solution (FP2) maintains the stability of the stable eigenvalue $-4/9$. However, the

nontrivial solution vanishes and the response jumps into the trivial solution (FP1) as σ is increased to 0.2 at $n = 30$. The trivial solution after $n = 30$ exhibits a strong stability, that is, it is not randomly fluctuated and seems to maintain the constant value $r_n = 0$ while the original system (1) is randomly fluctuated by A_n.

This example makes it clear that the synchronization we consider can not be characterized by the deterministic stability analysis because the difference between the synchronized and the unsynchronized solutions can not be characterized by the same eigenvalue.

3 The Markov process generated by discrete maps

As another option to characterize the synchronization, we derive a recursion formulae which determines the transition probability densities of the stochastic system (1).

3.1 The single map case

We start with the simplest case, that for the single logistic map with the random coefficient A_n of the form:

$$x_{n+1} = A_n x_n (1 - x_n). \tag{4}$$

Let $p^n(x)$, $p^{n+1}(x)$, $\rho(A)$ be the probability density function (PDF) of x_n, x_{n+1}, A_n respectively, and suppose that $p^n(x)$ is known, $\rho(A)$ is known and stationary, and $p^n(x)$ and $\rho(A)$ are independent. To avoid singularity, we also assume the condition $0 < x_n < 1$ without loss of generally because the trivial solutions $x = 0, 1$ are not of interest in our investigation. Then, the unknown density $p^{n+1}(x)$ is determined as follows[16].

We first introduce the transformation:

$$x_{n+1} = A_n x_n (1 - x_n),\ y = x_n,$$

whose Jacobian is given by

$$\frac{\partial(x_{n+1}, y)}{\partial(A_n, x_n)} = x_n(1 - x_n).$$

From the assumption $0 < x < 1$, the transformation is holomorphic so that the unknown joint PDF, $p(x_{n+1}, y)$ can be determined by the known $p(A_n, x_n) = \rho(A)p^n(x)$

as

$$p(x_{n+1}, y) = \left(\frac{\partial(x_{n+1}, y)}{\partial(A_n, x_n)} \right)^{-1} p^n(x)\rho(A).$$

Integrating it from 0 to 1 with respect to y, the desired $p^{n+1}(x)$ is obtained as the marginal PDF of $p(x_{n+1}, y)$,

$$\begin{aligned} p^{n+1}(x) &= \int_0^1 p(x_{n+1}, y)dy \\ &= \int_0^1 \frac{p^n(y)}{y(1-y)} \rho\left(\frac{x}{y(1-y)} \right) dy. \end{aligned} \tag{5}$$

Therefore, the transition law from $p^n(x)$ to $p^{n+1}(x)$ is obtained as the recursion formulae (5) which governs the Markov process generated by the map (4).

3.2 The linked pair case

Such a transformation of PDF also leads to the transition law of the synchronization system (1), however, some additional trick is needed in this case. We thus start with the unlinked form:

$$\begin{aligned} x_{n+1} &= A_n x_n(1 - x_n), \\ y_{n+1} &= B_n y_n(1 - y_n) \end{aligned} \tag{6}$$

Let $p^n(x, y)$ be the joint probability density of x_n and y_n, and $\rho(A, B)$ be that of A_n and B_n, and suppose that the response is independent of the input at the same time, i.e., $p(x_n, y_n, A_n, B_n) = p(x_n, y_n)\rho(A, B)$, and that ρ is stationary. Then, we introduce the following transformation:

$$\begin{aligned} x_{n+1} &= A_n x_n(1 - x_n), \\ y_{n+1} &= B_n y_n(1 - y_n), \\ u &= x_n, \quad v = y_n \end{aligned}$$

whose Jacobian is

$$\frac{\partial(x_{n+1}, y_{n+1}, u, v)}{\partial(x_n, y_n, A_n, B_n)} = x_n y_n(1 - x_n)(1 - y_n).$$

It is clear that the transformation is holomorphic in the domain $0 < x_n, y_n < 1$, so

that

$$p(x_{n+1}, y_{n+1}, u, v) = \frac{p^n(u,v)}{uv(1-u)(1-v)}\rho\left(\frac{x_{n+1}}{u(1-u)}, \frac{y_{n+1}}{v(1-v)}\right).$$

Integrating $p(x_{n+1}, y_{n+1}, u, v)$ from 0 to 1 with respect to u and v, we obtain the recursion formulae:

$$p^{n+1}(x,y) = \int_0^1 \int_0^1 \frac{p^n(u,v)}{uv(1-u)(1-v)} \times \rho\left(\frac{x}{u(1-u)}, \frac{y}{v(1-v)}\right) dudv. \tag{7}$$

To rewrite the unlinked form (7) to the linked form corresponding to the linked pair of maps (1), we assume the joint density $\rho(A, B)$ of the form:

$$\rho(A,B) := \rho(A)\delta(A-B) = \rho(B)\delta(A-B) \tag{8}$$

where the probability density $\rho(A)$ of A_n and $\rho(B)$ of B_n are assumed to be identical, i.e., $\rho(A) = \rho(B)$, and δ is the Dirac's delta function with the following properties[17]:

(d1) $\delta(-x) = \delta(x)$,
(d2) $f(x)\delta(x-a) = f(a)\delta(x-a)$,
(d3) $\delta(ax) = |a|^{-1}\delta(x)$, more generally,

$$g(x_i) = 0 \quad (i = 1, 2, \cdots, n) \Longrightarrow \delta(g(x)) = \sum_{i=1}^{n} |dg(x_i)/dx|^{-1}\delta(x - x_i).$$

From the definition (8), the probability of the event $A_n \neq B_n$ equals 0 and the marginal density of it is identical to the density $\rho(A) = \rho(B)$, that is,

$$\int_{-\infty}^{\infty} \rho(A,B)dA = \rho(A) = \rho(B) = \int_{-\infty}^{\infty} \rho(A,B)dB.$$

This means that the value of the random variable A_n is identical to that of B_n with probability 1, and thus the assumption (8) reasonably corresponds to the situation where the pair of maps is linked by the common noise A_n, as defined in (1).

Then, the linked version of (7) is obtained in the form:

$$p^{n+1}(x,y) = \int_0^1 \int_0^1 \frac{p^n(u,v)}{uv(1-u)(1-v)} \times \rho\left(\frac{x}{u(1-u)}\right)\delta\left(\frac{x}{u(1-u)} - \frac{y}{v(1-v)}\right) dudv. \tag{9}$$

Applying (d1)-(d3) to eliminate the delta function from (9), we finally obtain the recursion formulae:

$$p^{n+1}(x,y) = \int_0^1 \rho\left(\frac{x}{v(1-v)}\right) \times \frac{p^n\left(\frac{1}{2}(1-\Phi),v\right) + p^n\left(\frac{1}{2}(1+\Phi),v\right)}{y\Phi} dv \tag{10}$$

where $\Phi := \Phi(x,y,v) = \sqrt{1-4xv(1-v)/y}$.

The recursion formulae (10) describes the transition law from $p^n(x,y)$ to $p^{n+1}(x,y)$. This means that the error among the synchronization system (1) generates the Markov process governed by (10).

4 Probability densities of the synchronization

4.1 A special solution for the perfect synchronization

We first assume a candidate of a stationary solution of the equation (10) of the following form:

$$p^n(x,y) := \delta(x-y)p^n(x) = \delta(x-y)p^n(y)$$

where $p^n(x)$ is a solution of the equation (5) which is the state probability density of the single map (4) at the time n.

Put, $\alpha := x/y$, and

$$\begin{aligned} g_1 &:= \frac{1}{2}(1-\Phi) - v, \quad g_2 := v - \frac{1}{2}(1+\Phi), \\ p_1^n &:= p^n\left(\frac{1}{2}(1-\Phi),v\right) = \delta(g_1)p^n(v), \\ p_2^n &:= p^n\left(\frac{1}{2}(1+\Phi),v\right) = \delta(g_2)p^n(v), \end{aligned}$$

where $\Phi(x,y,v) = \Phi(\alpha,v) = \sqrt{1-4\alpha v(1-v)}$. Then, zeros of $g_i = g_i(\alpha)$ are obtained as a simple point $\alpha = 1$ ($i = 1,2$), and the derivative of $g_i(\alpha)$ is

$$g_i'(\alpha) = g'(\alpha) = \frac{2v(1-v)}{\sqrt{1-4\alpha v(1-v)}}.$$

Therefore, from (d1)-(d3), we can rewrite p_1^n, p_2^n as

$$p_i^n = \frac{1}{|g_i'(1)|}\delta(x/y-1)p^n(v) = \frac{|y|}{|g_i'(1)|}\delta(x-y)p^n(v)$$
$$= \frac{y\sqrt{1-4v(1-v)}}{2v(1-v)}\delta(x-y)p^n(v) \quad (i=1,2). \tag{11}$$

Substituting (11) into (10), we have

$$p^{n+1}(x,y) = \delta(x-y)$$
$$\times \int_0^1 \rho\left(\frac{y}{v(1-v)}\right)\frac{p^n(v)\sqrt{1-4v(1-v)}\,dv}{v(1-v)\sqrt{1-4v(1-v)^{\frac{x}{y}}}}.$$

Since $\delta(x-y)=0$ if $x \neq y$,

$$= \delta(x-y)$$
$$\times\left(\int_0^1 \rho\left(\frac{y}{v(1-v)}\right)\frac{p^n(v)\sqrt{1-4v(1-v)}\,dv}{v(1-v)\sqrt{1-4v(1-v)^{\frac{x}{y}}}}\right)_{x=y}$$
$$= \delta(x-y)\int_0^1 \rho\left(\frac{y}{v(1-v)}\right)\frac{p^n(v)}{v(1-v)}dv.$$

From the equation (5), finally we have

$$= \delta(x-y)p^{n+1}(y).$$

Therefore, it is proved that $\delta(x-y)p^n(y)$ is a special solution of the equation (10).

This special solution exactly corresponds to the perfect synchronization of x_n and y_n in the system (1) because from the definition of the delta function, the probability of the event, $r_n = x_n - y_n \neq 0$, equals 0 and the density of unit volume is perfectly concentrated on the line $r_n = x_n - y_n = 0$. In other words, values of the random variables x_n and y_n are perfectly synchronized with probability 1.

4.2 Numerical examples

Figure 4 shows the transient probability densities of the synchronization system (1) obtained by Monte Carlo simulations over 2×10^7 samples of the numerical solution of (1) starting from $(x_0, y_0) = (\frac{13-\sqrt{13}}{20}, \frac{13+\sqrt{13}}{20})$ which corresponds to one of the nontrivial solutions (FP2).

As the time n is increased, the initial density concentrated at the initial point (x_0, y_0) becomes diffused around. Meanwhile, a part of diffused density becomes captured

by the peak on the line $r_n = x_n - y_n = 0$. The diffused density nearly vanishes until $n = 2000$ and only the peak of the form $\delta(x-y)p^n(y)$ becomes alive.

This numerical result provides a phenomenological evidence of the stationary density of the form $\delta(x-y)p^n(y)$ generated by the synchronization system (1), and thus the analytical result is confirmed. To this end, we can reasonably conclude that the perfect synchronization corresponding to the trivial solution (FP1), $r_n = x_n - y_n = 0$ can be identified as an absorbing barrier of the Markov process. In view of this, the nontrivial solution (FP2) can be regarded as local minima having a potential higher than that of the trivial solution confined on the absorbing barrier.

5 Mean escape times under chaotic bifurcations

What has been probed in the section 4.1 is independent of the density of A_n. In other words, the existence of the perfect synchronization does not depends on the parameters A_c and σ. The implication is that the synchronization system (1) may produce the perfect synchronization even in the chaotic region of the logistic map. However, the proof guarantees the existence only, so that the global stability of the solution $\delta(x-y)p_n(y)$ is unknown yet. In particular, the extent of the basin of attraction of the absorbing barrier $x = y$ directly affects applicability of the synchronization to physical situations. From this point of view, we finally investigate escape times to reach the absorbing barrier $\delta(x-y)p_n(y)$. The escape times are supposed to be roughly in inverse proportion to the extent of attraction.

Figure 5 shows the mean escape time $\langle n(x_0, y_0)\rangle$ for $\sigma = 0.2$ and $A = 10/3, 3.6$ where $n(x_0, y_0)$ represents the escape time in which a sample starting from (x_0, y_0) reaches the absorbing barrier $x = y$. Symmetric parts with respect to the line $x = y$ are omitted in the plots. The average $\langle\cdots\rangle$ is taken over 2×10^4 samples of the numerical solution (x_n, y_n) $(1 \le n \le 2000)$ of (1). The initial points are placed on the uniform 60×60 grids on the rectangle region $(0, 1) \times (0, 1)$. For numerical representation of the equality $x_n = y_n$, the criterion $|x_n - y_n| < 10^{-15}$ is applied.

For $A_c = 10/3$, the maximal mean escape time is estimated as $\max_{(x_0,y_0)} \langle n(x_0, y_0)\rangle \approx 544.18 < 555$. Thus, all of the averaged responses of different initial conditions reaches the absorbing barrier before $n = 555$. We can detect a set of zeros of $\langle n(x_0, y_0)\rangle$ along the line $x_0 - y_0 = 0$ which corresponds to the perfect synchronization. This synchronizing set is surrounded by the steep wall of a ravine like shape. The wall is ended by a flat part of the height $\langle n(x_0, y_0)\rangle \approx 120$. The flat part is divided into several parts by oblique prisms like rises being placed symmetrically with respect to the centre $(0.5, 0.5)$. These rises imply that the extent of attraction of the barrier $x_n - y_n = 0$ as a function of (x_0, y_0) has local minima. In particular, the right hand side of the larger two rises covers the two-periodic solution which causes the transient peak of densities as shown in Figure 4 for $n = 40$. Besides all this, it

is also important to note that there is the second ravine along the line $x_0 + y_0 = 1$.

The second ravine implies the existence of lower dimensional dynamics along which it takes a few iterations to reach the absorbing barrier. Indeed, the numerical estimation of the escape time $n(x_0, y_0)$ along the line $x_0 + y_0 = 1$ is obtained as

$$n(x_0, y_0)|_{x_0+y_0=1} = \begin{cases} 0, & \text{if } x_0 = y_0, \\ 1, & \text{otherwise} \end{cases} \tag{12}$$

for all of 2×10^7 samples of the excitation. It follows numerically that $n(x_0, y_0)$ is not random any more on the line $x_0 + y_0 = 1$ and becomes the deterministic function which is locally constant in the domain $\{(x_0, y_0) \mid x_0 + y_0 = 1,\ x_0 \neq y_0\}$. Analytical explanation of it can easily be obtained by the trivial fact: for any x_n, y_n, A_n, the condition $x_0 + y_0 = 1$ gives

$$y_{n+1} = A_n y_n (1 - y_n) = A_n (1 - x_n) x_n = x_{n+1}. \tag{13}$$

Therefore, it is numerically and analytically shown that there exists the lower dimensional dynamics where all the initial points on the line $x_0 + y_0 = 1$ reach the synchronizing set $x_0 - y_0 = 0$ in the unit step of iterations. It must be noted that this flow from points on $x_0 + y_0 = 1$ to the perfect synchronization is not stochastic because of the deterministic law (13).

As A_c is increased to $A_c = 3.6$, the sample path becomes chaotic, that is, the chaotic bifurcation occurs. This is because the condition $A_c = 3.6$ is within the chaotic region of the logistic map already shown in Figure 1. First of all, as shown in Figure 5 for $A_c = 3.6$, the first ravine along the synchronizing set $x_0 - y_0 = 0$ maintains even in the chaotic region, showing that the analytical result is also valid for the chaotic case. It is also found that the second ravine along $x_0 + y_0 = 1$ maintains in the chaotic region because of the fact (13).

In the chaotic region, however, ripples of $\langle n(x_0, y_0) \rangle$ disappear and the set of initial conditions can be divided into only the three parts: the flat of the maximal height $\langle n(x_0, y_0) \rangle = 2000$, the first ravine along $x_0 - y_0 = 0$ of zero height, and the second ravine along $x_0 + y_0 = 1$ of unit height. This means that the extent of attraction hardly depends on the initial conditions in this time interval, that is, all the initial conditions out of the ravines can not reach the synchronizing set $x_0 - y_0 = 0$ by the maximal iterations of this simulation.

The above result on the escape times makes it clear that the bifurcation from periodic to chaotic behaviour reduces the attraction of the absorbing barrier while it does not affect the existence of the perfect synchronization and the lower dimensional dynamics. In other words, the perfect synchronization exists even in the chaotic region but it is rarely produced by arbitrary initial points although the convergence to the perfect synchronization might be slightly accelerated by the lower

dimensional dynamics.

6 Experimental Synchronization

In order to provide an intuitive example of the synchronization in physical situations, we propose the circuit shown in Figure 6. The circuit consists of a pair of multivibrators of the same physical structure, which are linked by the common noisy input V_{in} only. The input V_{in} is a Gaussian white noise with zero mean. The root square mean voltage of V_{in} is is changed from 0 V(rms) to 0.3 V(rms) at $t = 40$s and from 0.3 V(rms) to 0 V(rms) at $t = 80$s. It should be noted that 0.3 V(rms) is 16.7% of the peak-to-peak voltages of the outputs V_x, V_y. The physical parameters are selected as $V_{cc} = 5$V, $C = 47\mu$F, $R_1 = 22$kΩ, $R_2 = 330\Omega$.

Figure 7 shows the experimental data of the output V_x, V_y of the pair of multivibrators. In the absence of noise before $t = 40$s, the multivibrators oscillate with slightly different periods due to experimental errors. In contrast, in the presence of noise from $t = 40$s, they rapidly become synchronize with each other while lower voltages of the outputs are randomly fluctuated by the noisy input V_{in}. When the noisy input is removed at $t = 80$, the multivibrators oscillate with slightly different periods again.

The most important point here is that the synchronization is nearly perfect even in this experimental situation. Although we have to note that our analytical model based on logistic maps is too simple to explain this experimental synchronization, we believe that our circuit provides an intuitive example to understand how to construct the perfect synchronization in physical uncoupled systems linked by external noisy inputs only. Further experimental investigation based on more precise models will be shown in our future studies.

7 Summary and concluding remarks

We have demonstrated that the pair of identical uncoupled logistic maps can perfectly be synchronized when they share the same noisy excitation and shown analytically that the pair generates the Markov process having the special solution of the form $\delta(x - y)p^n(y)$. The special solution can be regarded as the absorbing barrier of the Markov process which corresponds to the perfect synchronization. To evaluate the extent of attraction of the absorbing barrier, we have numerically estimated the mean escape time to reach the barrier as a function of the initial conditions. The result shows that the special solution maintains under chaotic bifurcation whereas the probability to reach the absorbing barrier is significantly decreased in

the chaotic region. In addition, we have also found that there is the lower dimensional dynamics along the line $x_0 + y_0 = 1$ on which all the initial points reach the perfect synchronization in the unit step of iterations.

From these results, we can reasonably conclude that the presence of the perfect synchronization of the uncoupled logistic maps linked by the common noisy excitation has been guaranteed both analytically and numerically in a stochastic manner.

Our recursion formulae (10) will provide a new analytical tool to investigate the synchronization of logistic maps. Because the recursion formulae (10) describes not only the stationary density $\delta(x - y)p(y)$ but also transient densities converging to the perfect synchronization $\delta(x - y)p(y)$. Therefore, our result presenting the existence of the stationary solution only is just the first step toward future developments of stochastic methods related to the noise-induced synchronization. Solving the recursion formulae (10) for the transient densities might answer physical or industrial questions such as how to design the optimal synchronization in practical situations or how long it takes for the solution to reach the perfect synchronization. Although the Monte-Carlo method is still effective for this purpose, it consumes too much computational resources. In view of this, the main problem in the near future would be investigating how to obtain analytic or semi-analytic solutions of (10). Primitive numerical methods for the transient solution might encounter numerical instabilities because the solution must converge analytically to the delta-type stationary solution.

Finally, we have proposed a physical implementation of the synchronization as the pair of multivibrators linked by the common noisy excitation only. The result clearly shows that it is possible to produce the noise-induced perfect synchronization even in physical situations. We believe that our experimental technique directly provides a new method to synchronize, for example, initial states of independently coexisting oscillators of the same specification.

References

[1] L. M. Pecora, T. L. Carroll, Synchronization of chaotic systems, Phys. Rev. Lett. 64 (8) (1990) 821–824.

[2] L. M. Pecora, T. L. Carroll, Driving systems with chaotic signals, Phys. Rev. A 44 (4) (1991) 2374–2383.

[3] R. Toral, C. R. Mirasso, E. Hernández-García, O. Piro, Analytical and numerical studies of noise-induced synchronization of chaotic systems, Chaos 11 (3) (2001) 665–673.

[4] H. Suetani, T. Horita, S. Mizutani, Noise-induced enhancement of fluctuation and spurious synchronization in uncoupled type-I intermittent chaotic systems, Phys. Rev. E 69 (2004) 016219.

[5] A. Stefański, T. Kapitaniak, Synchronization of mechanical systems driven by chaotic or random excitation, J. Sound and Vibration 260 (2003) 565–576.

[6] C. S. Zhou, J. Kurths, E. Allaria, S. Boccaletti, R. Meucci, F. T. Arecchi, Constructive effects of noise in homoclinic chaotic systems, Phys. Rev. E 67 (2003) 066220.

[7] A. B. Neiman, D. F. Russell, Synchronization of noise-induced bursts in noncoupled sensory neurons, Phys. Rev. Lett. 88 (13) (2002) 138103.

[8] K. Yoshida, K. Sato, Noise-induced synchronization without coupling, Trans. JSME Series C (in Japanese) 70 (696) (2004) 2228–2234.

[9] H. Fujisaka, T. Yamada, Stability theory of synchronized motion in coupled-oscillator systems, Prog. Theor. Phys. 69 (1) (1983) 32–47.

[10] C. Kim, Mechanism of chaos synchronization and on-off intermittency, Phys. Rev. E 56 (1997) 3697–3700.

[11] A. S. Pikovsky, Statistics of trajectory separation in noisy dynamical systems, Phys. Lett. A 165 (1992) 33–36.

[12] L. Arnold, G. Bleckert, K. R. Schenk-Hoppe, The stochastic Brusselator: Parametric noise destroys Hopf bifurcation, in: Stochastic Dynamics, Springer-Verlag, 1999, pp. 71–92.

[13] K. Yoshida, K. Sato, Stochastic synchronization in self-excited systems, in: Proccedings of the 34rd ISCIE International Symposium on Stochastic Systems Theory and its Applications, October 31-November 1, 2002, Fukuoka, Japan, ISCIE, Kyoto, 2003, pp. 258–263.

[14] A. Maritan, J. R. Banavar, Chaos, noise, and synchronization, Phys. Rev. Lett. 72 (1994) 1451–1454; 73 (1994) 2931–2932.

[15] S. Rim, D. Hwang, I. Kim, C. Kim, Chaotic transition of random dynamical systems and chaos synchronization by common noises, Phys. Rev. Lett. 85 (2000) 2304–2307.

[16] A. Papoulis, Probability, Random Variables, and Stochastic Processes, McGraw-Hill, Singapore, 1984, pp. 123–148.

[17] P. A. M. Dirac, The Principles of Quantum Mechanics, Oxford University Press, London, 1958, pp. 58–61.

List of Figures

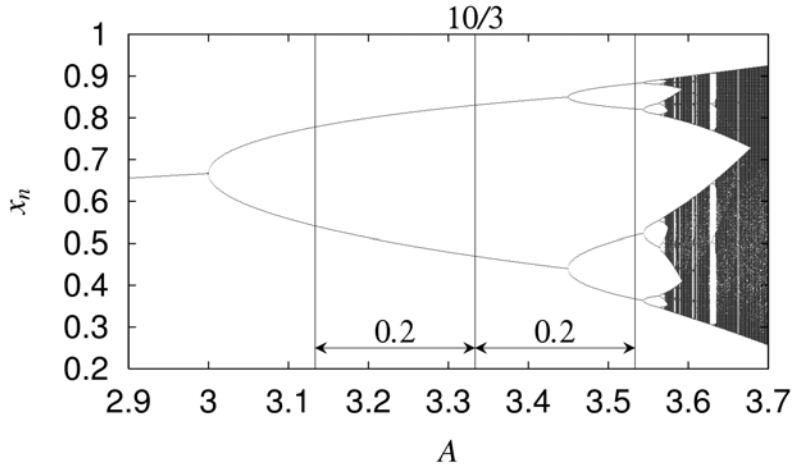

Fig. 1. Deterministic bifurcation diagram of logistic map.

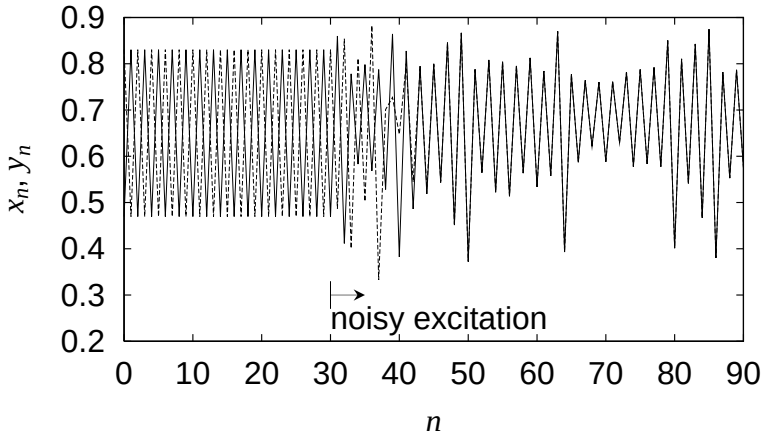

Fig. 2. Noise-induced synchronization of the pair of logistic maps linked by common noisy excitation where the noise intensity σ is changed from 0.0 to 0.2 at $n = 30$.

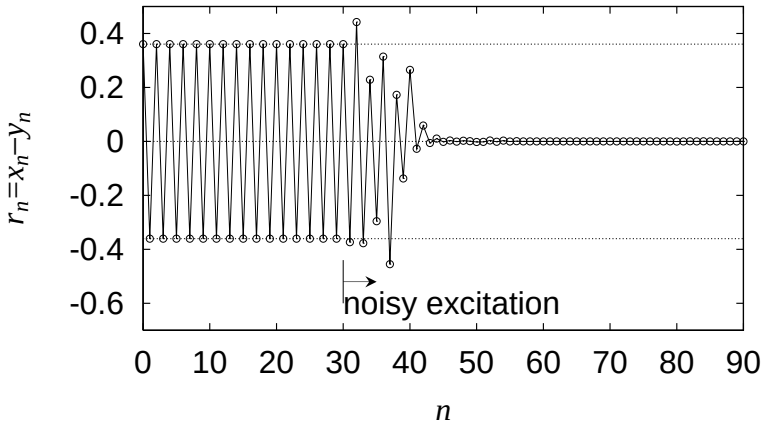

Fig. 3. A sample process of the error system for $A = 10/3$ where the noise intensity σ is changed from 0.0 to 0.2 at $n = 30$.

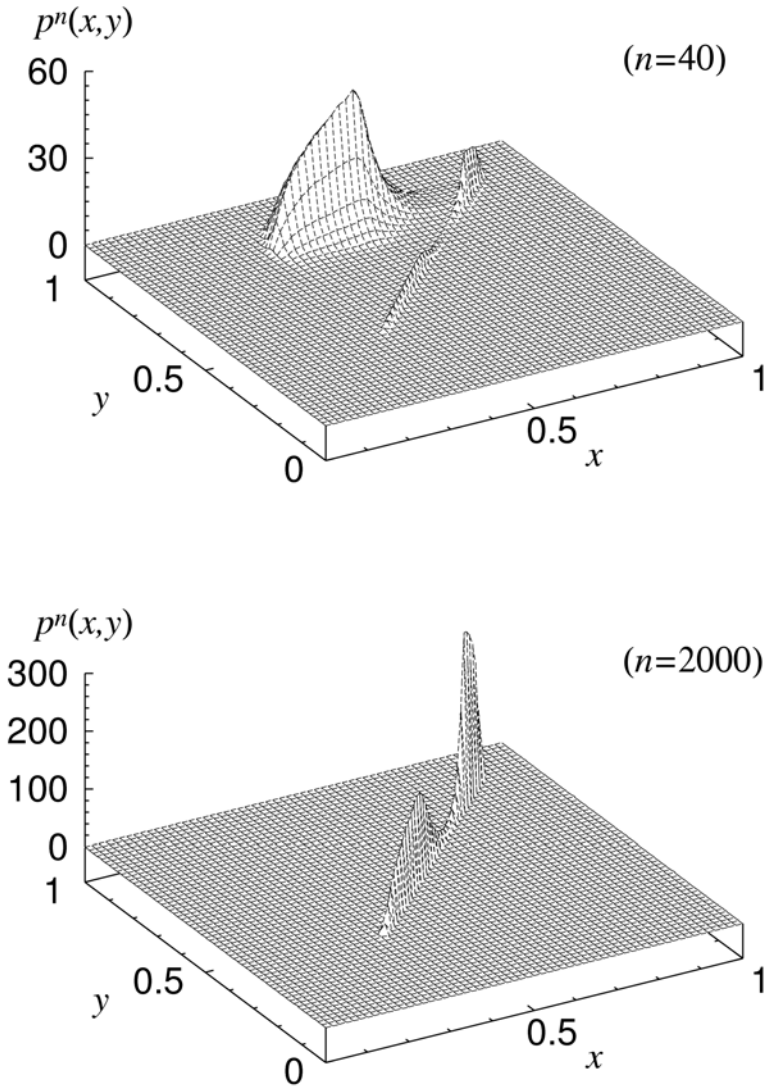

Fig. 4. Numerical transient probability densities of the pair of maps for $A = 10/3$, $\sigma = 0.2$ and for $n = 40, 2000$. The density is obtained from 10^7 samples of the numerical solution.

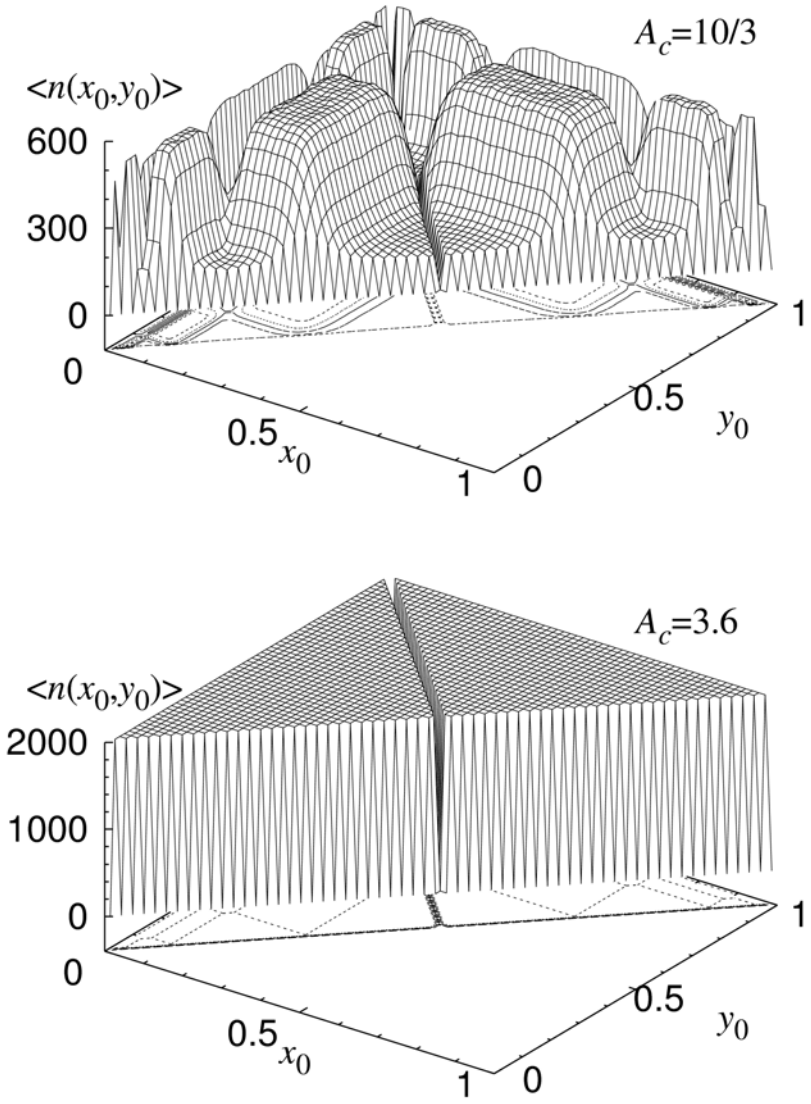

Fig. 5. Mean escape times to reach the absorbing barrier $x = y$, for $\sigma = 0.2$, and for $A_c = 10/3$ in the two-periodic region and $A_c = 3.6$ in the chaotic region. Each point to plot is obtained from 2×10^4 samples starting from the uniform 60×60 grid points. Symmetric parts with respect to the line, $x = y$, are omitted.

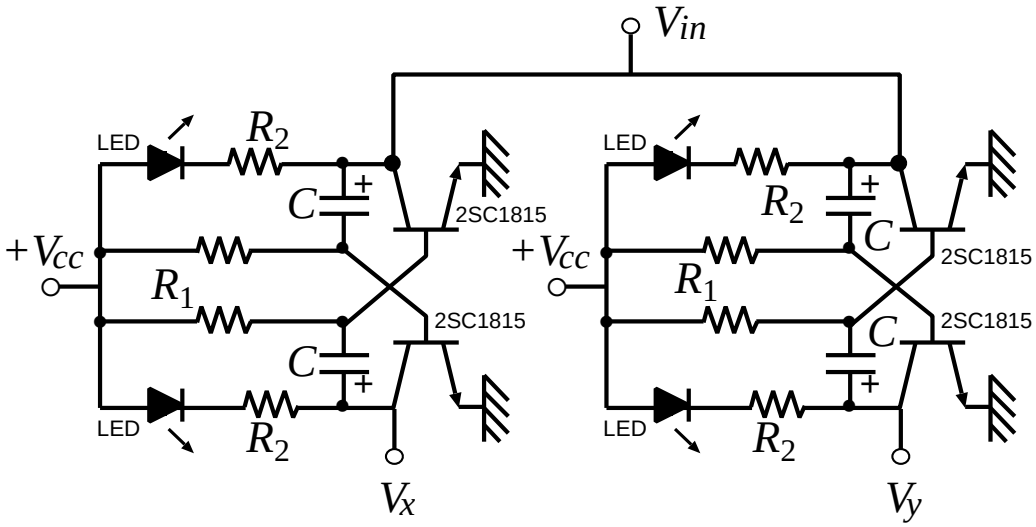

Fig. 6. The pair of multivibrators subjected to the common noisy input voltage V_{in}. The output voltages V_x and V_y are measured.

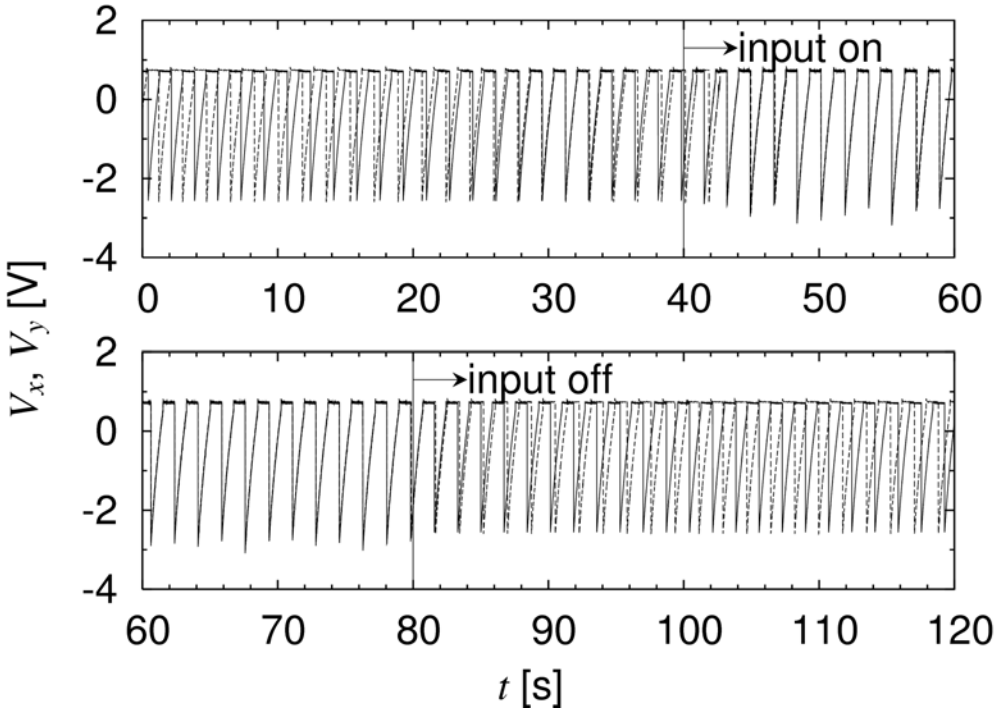

Fig. 7. Experimental synchronization in the pair of multivibrators. The noisy input V_{in} is applied from t = 40 to 80.